Polyhedron 104 (2016) 9–16

Contents lists available at ScienceDirect

Polyhedron

journal homepage: www.elsevier.com/locate/poly

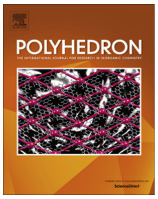

Chiral double helical silver complexes: subcomponent self-assembly and self-sorting

Feng-Li Zhang[a], Lei Tian[a], Long-Fang Qin[a], Jia-Qian Chen[a], Zaijun Li[a], Xuehong Ren[b], Zhi-Guo Gu[a,*]

[a] The Key Laboratory of Food Colloids and Biotechnology, Ministry of Education, School of Chemical and Material Engineering, Jiangnan University, Wuxi 214122, PR China

[b] The Key Laboratory of Eco-textiles of Ministry of Education, College of Textiles and Clothing, Jiangnan University, Wuxi 214122, PR China

ARTICLE INFO

Article history:
Received 28 September 2015
Accepted 30 October 2015
Available online 7 November 2015

Keywords:
Chiral complex
Double helicate
Silver complex
Subcomponent self-assembly
Self-sorting

ABSTRACT

Four homochiral dinuclear complexes, namely, $[Ag_2(L_{C4})_2](OTf)_2$ (**1**), $[Ag_2(L_{C4})_2](ClO_4)_2$ (**2**), $[Ag_2(L_{C5})_2](OTf)_2$ (**3**), $[Ag_2(L_{C5})_2](PF_6)_2$ (**4**) have been successfully synthesized from subcomponent self-assembly of imidazole-2-carboxaldehyde derivatives, *R*-phenylethylamine and silver salt. L_{C4} and L_{C5} were flexible ligands, containing the same imidazole Schiff-bases coordination motif and varying in alkyl chain lengths with four and five carbon atom, respectively. Single crystal structures revealed that the silver(I) center in **1**–**4** coordinated with 4 N donor atoms from two symmetrical chiral ligands assuming Δ configuration with a tetrahedral coordination environment. $[Ag_2(L_{Cn})_2]^{2+}$ components all presented double helical structures exhibiting only *P*-handedness with Ag–Ag, π–π, and C–H$\cdots\pi$ intramolecular interactions. Highly selective narcissistic self-sorting behavior can be observed during the self-assembly of **1** and **3**.

1. Introduction

Chiral polynuclear complexes have received a great deal of attention because of their utility in asymmetric catalysis, chiral separation, and nonlinear optical and magnetic properties [1,2]. However, the difficulties of maintaining chiral in crystallization process for polynuclear complexes make synthesis a predetermined chiral cluster structure rather challenging. Subcomponent self-assembly has become a well-established method for the construction of functional structures ranging in complexity from helicates to polynuclear cages [3]. Subcomponent self-assembly process involves the simultaneous formation of covalent and coordinate bonds, bringing both ligand and complex into being at the same time [4]. Subcomponent self-assembly not only reduces the effort required for ligand synthesis but also furnishes a means to create structures capable of dynamic rearrangement in solution [5]. One of the most special phenomena of subcomponent self-assembly is self-sorting [6]. Self-sorting and dynamic libraries of products prepared through subcomponent self-assembly are vital for the controlled formation of molecular constructs [7]. The ligands with a greater the difference in geometry, size, coordination angle, and coordination denticity, the easier the self-sorting becomes [8]. Most reported self-sorting systems are based on rigid components, while the self-sorting phenomenon with flexible components is few. When using flexible components with highly similar geometry and identical coordination motifs, mixed-ligand complex is most commonly obtained, and highly controlled narcissistic selectivity is rare observed.

To develop homochiral polynuclear compounds, we focused our attention on subcomponent self-assembly of di(imidazole aldehyde), chiral amine and transition metal ions [9]. In this particular self-assembly process, di(imidazole aldehyde) and chiral amine can easily generate bis-bidentate chiral Schiff-base ligands containing two N-imidazol and two N-amide donor groups, which can chelate multiple transition metal ions to form stable chiral polynuclear complexes. In this paper we report the synthesis of four homochiral silver dinuclear complexes through subcomponent self-assembly, and subsequently develop this system along self-sorting (Supporting information). Flexible ligands L_{C4} and L_{C5} are formed in situ, which displayed identical coordination geometry, and different lengths of central bridging alkyl chain (L_{C4} = 1,4-di((imidazol-2-ylmethylene)-1-phenylethanamine)butane, L_{C5} = 1,5-di((imidazol-2-ylmethylene)-1-phenylethanamine)pentane). Interestingly, highly selective narcissistic self-sorting can be achieved in the self-assembly process of the mixture of chiral phenylethylamine, AgOTf, and two different flexible di(imidazole aldehyde).

2. Experimental

2.1. Materials and methods

All reagents and solvents were reagent grade, purchased from commercial sources and used without further purification. *Caution:*

---

* Corresponding author. Tel.: +86 510 85917090; fax: +86 510 85917763.
E-mail address: zhiguogu@jiangnan.edu.cn (Z.-G. Gu).

http://dx.doi.org/10.1016/j.poly.2015.10.055
0277-5387/

The perchlorate salts are potentially explosive. Thus, these starting materials should be handled in small quantities and with great caution. Infrared spectra were measured on an ABB Bomem FTLA 2000-104 spectrometer with KBr pellets in the 500–4000 cm^{-1} region. NMR spectra were recorded on AVANCE III (400 MHz) instrument at 298 K using standard Varian or Bruker software, and chemical shifts were reported in parts per million (ppm) downfield from tetramethylsilane. Element analyses were conducted on elementar corporation vario EL III analyzer. UV–vis absorbance spectra were collected on Shimadzu UV-2101 PC scanning spectrophotometer. Circular dichroism (CD) spectra were carried out using a MOS-450/AF-CD spectro polarimeter at room temperature, which were calibrated conventionally using 0.060% ACS for intensity and a holmium filter for wavelength. ESI-MS spectra were recorded on a Waters Maldi Synapt Q-TOF Mass Spectrometer fitted with electrospray ionization. Samples were analyzed by direct infusion at 10 μL/min and scanned in the m/z range 100–1500. In the positive-ion mode the following conditions were used: capillary, 3.0 kV; cone, 30 V; source block temperature, 100 °C; desolvation temperature, 400 °C; cone and desolvation gas (N_2), 50 and 500 L/h, respectively.

2.2. Preparation of the complexes

2.2.1. 1,4-Di(imidazole-2-carboxaldehyde)butane

This compound was previously reported and prepared following the same procedure [9].

2.2.2. 1,5-Di(imidazole-2-carboxaldehyde)pentane

A mixture of imidazole-2-carboxaldehyde (1.35 g, 14 mmol), 1,5-dibromopentane (1.15 g, 5 mmol), potassium carbonate (1.38 g, 10 mmol), and 25 mL DMF were added to a flask in nitrogen atmosphere. The reaction mixture was stirred at 50 °C for 3 days. After cooling to room temperature the reaction mixture was filtered to get yellow solution. The filtrate was extracted with ethyl acetate (4 × 10 mL). The collected organic phase was washed with saturated aqueous solution of potassium chloride, and dried with anhydrous magnesium sulfate. After removing the solvent on a rotary evaporator, the residue was dried under vacuum at 40 °C overnight to get the desired product as yellow powder (Yield: 1.03 g, 79%). Pale yellow crystals of 1,5-di(imidazole-2-carboxaldehyde)pentane were obtained by recrystallizing the crude product from ethyl acetate. Elemental analysis (%) calc. for $C_{13}N_4H_{16}O_2$: C, 59.99; N, 21.52; H, 6.20. Found: C, 59.98; N, 21.49; H, 6.22. IR (KBr, ν cm^{-1}): 3122, 2997, 2894, 1685, 1485, 1417, 286, 771. ^{1}H NMR (400 MHz, CD_3CN, δ ppm): 9.68 (s, 2H), 7.35 (s, 2H), 7.24 (s, 2H), 4.37 (t, J = 8.5 Hz, 4H), 1.80 (m, 4H), 1.43 (m, 2H).

2.2.3. Complex $[Ag_2(L_{C4})_2](OTf)_2$ (**1**)

1,4-Di(imidazole-2-carboxaldehyde)butane (24.6 mg, 0.1 mmol), (R)-1-phenylethylamine (24.2 mg, 0.2 mmol), and AgOTf (25.7 mg, 0.1 mmol) were added to a flask with 10 mL acetonitrile. The solution was heated at 80 °C for 2 h, cooled to room temperature, and then stirred for further 2 h. After adding 5 mL methanol and 10 mL·H_2O the reaction solution was filtered. Complex **1** was precipitated as colorless crystals through slow evaporation of the filtrate at room temperature for 2 weeks. Yield: 69%. Elemental analysis (%) calc. for $Ag_2C_{58}N_{12}H_{66}F_6S_2O_7$: C, 48.47; N, 11.70; H, 4.63. Found: C, 48.23; N, 11.95; H, 4.68. UV–vis (CH_3CN, λ_{max}, nm): 208, 286. IR (KBr, ν cm^{-1}): 3117, 3030, 2970, 2920, 2870, 1632, 1450, 1369, 1261, 1157, 1088, 1032, 953, 837, 760, 702, 636, 555. ^{1}H NMR (400 MHz, CD_3CN, δ ppm): 8.22 (s, $2H^6$), 7.45 (t, J = 29.4 Hz, $2H^1$), 7.29 (d, J = 22.4 Hz, $4H^3$), 7.20 (t, J = 7.6 Hz, $4H^2$), 6.73 (s, $2H^7$), 5.04 (m, $2H^8$), 4.76 (q, J = 14.1 Hz, $2H^4$), 4.42 (d, J = 14.3 Hz, $2H^9$), 3.79 (t, J = 13.5 Hz, $2H^{12}$), 1.47 (d, J = 8.7 Hz, $6H^5$), 1.25 (m, $4H^{10,11}$).

2.2.4. Complex $[Ag_2(L_{C4})_2](ClO_4)_2$ (**2**)

This complex was prepared following a procedure similar to that for complex **1** except that $AgClO_4{\cdot}H_2O$ (22.5 mg, 0.1 mmol) instead of AgOTf was used. Colorless crystals of complex **2** were obtained with 85% yield. Elemental analysis (%) calc. for $Ag_2C_{58}N_{13}H_{67}Cl_2O_8$: C, 51.19; N, 13.38; H, 4.96. Found: C, 51.08; N, 13.45; H, 4.82. UV–vis (CH_3CN, λ_{max}, nm): 209, 288. IR (KBr, ν cm^{-1}): 3130, 3028, 2968, 2922, 1632, 1448, 1280, 1090, 955, 908, 845, 764, 700, 623, 548. ^{1}H NMR (400 MHz, CD_3CN, δ ppm): 8.23 (s, $2H^6$),

Table 1
Summary of crystallographic data for the complexes **1**–**4**.

	1	**2**	**3**	**4**
Formula	$C_{58}H_{66}Ag_2F_6N_{12}O_7S_2$	$C_{58}H_{67}Ag_2Cl_2N_{13}O_8$	$C_{60}H_{68}Ag_2F_6N_{12}O_6S_2$	$C_{58}H_{68}Ag_2F_{12}N_{12}P_2$
Formula weight	1437.09	1360.89	1447.12	1438.92
T (K)	173(2)	173(3)	173(2)	173(2)
λ (Å)	0.71073	0.71073	0.71073	0.71073
Crystal system	Orthorhombic	Orthorhombic	Monoclinic	Monoclinic
Space group	$C222_1$	$C222_1$	C2	C2
a (Å)	13.1993(7)	13.4533(11)	18.7430(3)	17.992(3)
b (Å)	18.4304(9)	17.7521(14)	13.4253(18)	13.749(2)
c (Å)	26.1637(13)	25.4528(18)	15.4914(18)	15.246(3)
α (°)	90	90	90	90
β (°)	90	90	121.790(2)	121.390(4)
γ (°)	90	90	90	90
V ($Å^3$)	6364.8(6)	6078.7(8)	3313.3(7)	3223.3(10)
Z	4	4	2	2
D_{calc} (Mg/m^3)	1.5	1.487	1.451	1.483
μ (mm^{-1})	0.758	0.796	0.728	0.739
$F(000)$	2936	2792	1480	1464
θ(°)	3.01–25.39	3.03–25.38	3.06–25.36	3.07–25.42
Index ranges	$-15 \leqslant h \leqslant 15$, $-22 \leqslant k \leqslant 22$, $-31 \leqslant l \leqslant 31$	$-16 \leqslant h \leqslant 15$, $-21 \leqslant k \leqslant 19$, $-29 \leqslant l \leqslant 30$	$-18 \leqslant h \leqslant 22$, $-16 \leqslant k \leqslant 16$, $-18 \leqslant l \leqslant 17$	$-21 \leqslant h \leqslant 21$, $-16 \leqslant k \leqslant 16$, $-18 \leqslant l \leqslant 18$
Reflections collected	15516	13017	9085	9369
Goodness-of-fit (GOF) on F^2	1.053	1.215	1.053	1.022
R_1^a, wR_2^b ($I > 2\sigma(I)$)	0.0402, 0.1012	0.0629, 0.1708	0.0536, 0.0782	0.0642, 0.0878
R_1^a, wR_2^b (all data)	0.0654, 0.1127	0.0916, 0.1879	0.1113, 0.0865	0.1319, 0.1006

$R_1^a = \Sigma||F_o| - |F_c||/\ \Sigma|F_o|$. $wR_2^b = [\Sigma w(F_o^2 - F_c^2)^2/\Sigma w(F_o^2)]^{1/2}$.